A R C H I V E S O F M E T A L L U R G Y A N D M A T E R I A L S
Volume 51 2006 Issue 4

J. DUTKIEWICZ* , J. MORGIEL*, L. LITYŃSKA-DOBRZYŃSKA*, W. MAZIARZ*, T. CZEPPE*, M. PARRA CARILLO*, T. B. MASSALSKI**

SEARCH FOR NEW METALLIC GLASS COMPOSITIONS IN NiZrTi BASE ALLOYS NEAR MULTICOMPONENT EUTECTIC POSITIONS

POSZUKIWANIE NOWYCH SKŁADÓW SZKIEŁ METALICZNYCH W STOPACH NA OSNOWIE NiZrTi W POBLIŻU WIELOSKŁADNIKOWYCH EUTEKTYK

In the present study several multicomponent alloys based on zirconium and nickel has been investigated. In the alloy containing Ni25Cu25Zr25Ti25 (all compositions in at. %) the position of the eutectic was identified as Ni29.2Cu29.9Zr17Ti24.9 and the melt spun alloy of this composition has shown a better glass forming ability than other alloys, as manifested by ΔT and T_{rg} increase. The four component alloy was modified by manganese addition and in this case the composition of the eutectic was identified at Ti21Zr14Ni27Cu27Mn7. The melt spun alloy has shown slightly better ΔT and T_{rg} than the initial alloy. Second copper rich eutectic was also identified in this system near Ti16Zr14Ni24Cu39Mn7 showing also $T_{rg.}$ = 0.63. Nickel rich alloy of composition Ni60Nb15Zr15Ti10 has shown primary Ni and Ti rich crystals and the eutectic identified at composition Ni48,5Nb21,5-Ti16.5Zr13,5. The eutectic alloy possess higher crystallization temperature (556°C) than the former one (545°C). TEM studies did not allow to find nanocrystals within the ribbon of the latter alloy. The four component eutectic has been modified by silicon addition and the alloy Ni45Nb21Ti16Zr13Si5 has been cast into an iron mould and melt spun. The alloy has been proved amorphous, however small crystallization peaks were found using DSC at 520°C, while the alloy of eutectic composition containing Ni50.3Nb14.4Ti17.3Zr15.1Si2.8 has shown crystallization temperature at 555°C and well pronounced T_g effect. The TEM studies did not allow to find nanocrystalls in the melt spun eutectic alloy, while crystals of size 1-2 nm were observed in the first alloy. Additions of a fifth element Mn to TiNiZnNi alloy and Si to the NiTiZrNb alloy do not clearly improves glass forming ability of the quintenary eutectics as compared to the quaternary ones.

Keywords: NiCuZrTiMn amorphous alloys NiNbTiZrSi alloys, glass forming ability

W niniejszej pracy przebadano kilkanaście stopów wieloskładnikowych na osnowie cyrkonu i niklu W stopie zawierajacym Ni25Cu25Zr25Ti25 skład eutektyki został określony jako Ni29.2Cu29.9Zr17Ti24.9 i stop o tym skladzie odlany na wirującym walcu wykazał lepszą skłonnośc do tworzenia szkła posiadając wyższe współczynniki ΔT i T_{rg}. Do eutektycznego stopu czteroskładnikowego dodano mangan. Skład eutektyki został określony jako Ti21Zr14Ni27Cu27Mn7. Po odlaniu na wirującym walcu stop eutektyczny wykazywał wyższe wskaźniki ΔT i T_{rg} jak stop odlany pierwotnie. Drugą eutektykę w tym systemie zidentyfikowano przy składzie Ti16Zr14Ni24Cu39Mn7 uzyskując dla taśmy T_g/T_L = 0.63.

Stop bogaty w nikiel o składzie Ni60Nb15Zr15Ti10 wykazywał po odlaniu kryształy pierwotne wzbogacone w Ni i Ti. Określono skład eutektyki jako Ni48,5Nb21,5-Ti16.5Zr13,5. Odlane taśmy stopu o tym składzie wykazują wyższą temperaturę krystalizacji (556°C) jak stop poprzedni (545°C). Badania TEM nie wykazały w stopie eutektycznym obecności nanokryształów w przeciwieństwie do pierwszego stopu. Stop eutektyczny czteroskładnikowy został zmodyfikowany przez dodatek krzemu i odlano na wirującym walcu stop o składzie Ni45Nb21Ti16Zr13Si5, który wykazał strukturę amorficzną podobnie jak czteroskładnikowy, krystalizując przy 520°C. Określono skład eutektyki o składzie Ni50.3Nb14.4Ti17.3Zr15.1Si2.8 która odlana w postaci taśmy wykazała krystalizację przy 555°C i wyraźny efekt T_g. Badania TEM stopu eutektycznego nie wykazały obecności nanokryształów w taśmach w przeciwieństwie do stopu pierwszego. Dodatki piątego pierwiastka nie wykazały wyraźnej poprawy skłonności do tworzenia szkieł w eutektyce pięcioskładnikowej w stosunku do stopów czteroskładnikowych.

* 1 INSTITUTE METALLURGY AND MATERIALS, POLISH ACADEMY OF SCIENCES, 30-059 KRAKÓW, 25 REYMONTA STR., POLAND
** CARNEGIE MELLON UNIVERSITY, 15213 PITTSBURGH, USA

1. Introduction

Search for new multicomponent eutectic compositions was initiated several years ago in the AgCuGe and CuTiZr systems [1, 2] in order to find new potential metallic glasses. This approach is based on the concept of the T_0 temperature introduced by M a s s a l s k i [3]. In the context of a phase diagram, for an alloy of composition c, T_0 is the temperature at which any two competing phases, say α and L, have the same free energies, i.e. $G_\alpha = G_L$. Below T_0, there is a driving force to transform L to α on cooling, provided that α remains of the same composition as L. Above T_0, the reverse is true. So, the T_0 line on the phase diagram represents the thermodynamic limit of a single-phase to single-phase transformation which is compositionally invariant and therefore partitionless. The important condition necessary for obtaining a partitionless transformation is a high cooling rate. In the case of a slow rate of cooling, an equilibrium α phase is formed from the melt, while when the cooling rate is higher, i.e. when we are able to supercool the liquid below T_0, but above the glass transition temperature T_g, a metastable crystalline α-solid solution may be obtained and this may compete with glass formation. If the liquid is supercooled below T_g, the amorphous structure of the liquid is preserved in the solid state. Hence, in order to prevent metastable partitionless crystallization before T_g is reached on cooling, alloys with compositions in the range of deep eutectics, with steeply falling T_0 curves, should be explored because the T_0 in such eutectics may lie below the T_g temperature.

The metallic glasses are characterized by a wide elastic range and a high strength approaching 2%, but accompanied by a very limited plasticity in compression and practically non in tension at ambient temperature [4, 5]. Various glasses show significant differences in mechanical properties therefore it is important to search for new compositions of potentially better plasticity.

The TiZrNiCu alloys of roughly equal amounts of alloying components turn out to be also relatively good glass former [6, 7]. The β-NiTi type precipitates form first during crystallization of TiZrNiCu in melt spun ribbons [7]. Considering previous results [1-3] the development of metallic glasses of improved plasticity from Ti - Zr - Ni - Cu system should take into account improvement of alloy glass forming ability near multicomponent eutectic compositions. In addition, considering the so called "confusion principle" [8] addition of other elements should help to obtain easy glass forming alloy by delaying crystallization. Among many possibilities of available alloying elements intended as minor additions to TiZrNiCu alloys aluminum is now of the additives, particularly in connection with zirconium base glasses [4-6]. The effectiveness of manganese, which often forms eutectics in binary systems, recently showed some improvement in glass forming ability [9]. However, these systems needs further studies.

Multicomponent NiTiZrCoNb nickel base amorphous alloys were obtained by rapid solidification [10, 11]. Bulk alloys exhibit a high elastic modulus, good corrosion resistance and compressive yield strength between 1,8 and 3 GPa with 2% fracture elongation. Surprisingly, $Ni_{59}Zr_{16}Ti_{13}Si_3Sn_2Nb_7$ as-cast BMG exhibits compressive plastic deformation of 6.5% before failure [12]. The bulk amorphous $Ni_{59}Zr_{20}Ti_{16}Si_2Sn_3$ alloy exhibits high

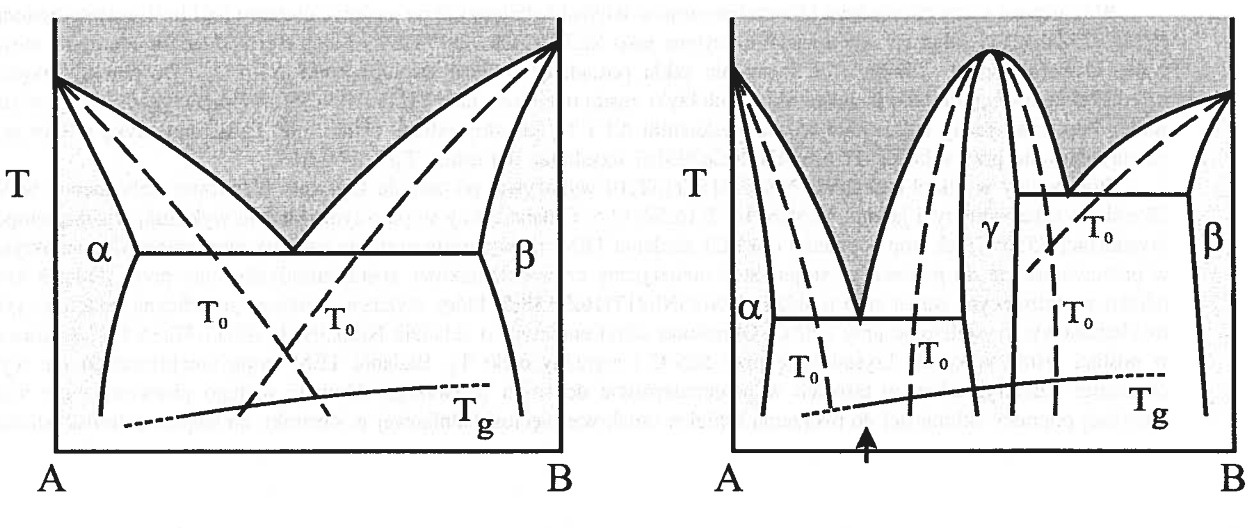

Fig. 1. Hypothetical phase eutectic binary diagrams showing changes of positions of T_0 and T_g curves in case of presence of an intermetallic compound

compressive fracture strength of about 2.7 GPa with a plastic strain of about 2% [13]. Due to reported positive effect of Nb and Si in this paper the development of a new amorphous alloys in the NiTiZrNbSi system prepared by rapid solidification was studied in relation to fine eutectic microstructure. Niobium forms high melting intermetalic phases with several elements, therefore as it can be seen in Fig. 1 there is a chance of obtaining steep T_0 curves and better chances to form metallic glass. The main effort of this study was centered on correlating the eutectic microstructure close to equilibrium with the glass forming ability in multicomponent systems containing 4-6 alloying additions. The glass forming ability was evaluated by $T_{gr} = T_g/T_l$ and $\Delta T_x = T_x - T_g$ and by microstructure studies and evaluation of the presence of nanocrystals within the amorphous matrix.

2. Experimental procedure

Alloys of compositions given in the Table 1 were melted in a Leybold induction furnace under argon atmosphere and cast into a steel mould ($\phi \sim 1$ cm, V ~20 cm^3) kept at 100°C. Small pieces of such ingots of volume of around 1 cm^3 were re-melted with high frequency currents in a quartz crucible with an 0.7 mm hole and the liquid alloy was ejected using 0,14 MPa helium pressure on a rotating copper wheel of diameter of 160 mm rotating with a linear rate between 8-24 m/s. The ribbons melt spun at 20 m/s were used to measure glass transition temperature T_g and crystallization temperature T_x. Above experiments were performed using differential scanning calorimeter (DSC) type Q1000 Thermal Analysis at a heating rate of 20 K/min. The melting temperatures were determined using differential thermal analysis (DTA) by Du Pont 1600 or Thermal Analysis Q600.

TABLE

The nominal compositions of investigated alloys

Alloy code	Chemical composition in at%						
	Ti	Nb	Zr	Ni	Cu	Mn	Si
G0	25		25	25	25		
G1-1	25		20	27.5	27.5	–	–
G1C	25		17	29	29	–	–
G1-7	25		20	22.5	22.5	10	–
G1-7A	23		18.5	25	28	5	–
G1-7AA	22		16	26	30	6	–
NNTZ-2	12.5	10	19.5	58	–	–	–
NNTZ-3	16.5	21.5	13.5	48.5			21.5
NNTZS5	16	21	13	45	–	–	5
NNTZS12	17.3	14.4	15.2	50.3	–	–	2.8

The microstructure observations were performed with either scanning electron microscopy XL30 equipped with X-ray energy dispersive (EDS) microanalysis system of ISIS Oxford Instrument or transmission electron microscope PHILIPS CM20 TWIN with EDAX Phoenix microanalysis attachment. The thin foil were prepared by double jet electro-polishing with nitric acetic mixed with alcohol at standard for such electrolyte conditions.

3. Results and discussion

Fig. 2 shows a part of quasiternary phase diagram TiZr(Cu + Ni) with marked compositions yielding amorphous structures during fast cooling. Two regions can be distinguished where a glass can be formed; one with majority of zirconium and the other with a large fraction of Ni + Cu. No relation to liquidus lines in the phase diagram is given like in the majority of works, where a search for new glasses was reported. The compositions investigated in the present work are also marked in this diagram (large gray circles). Fig. 3 shows SEM microstructures of alloys G0 (of equal content of all elements) outside the range marked by Lin and Johnson [13]. The microstructure in Fig. 3a shows dark primary crystals within multicomponent eutectic. The composition of the primary crystals measured using EDS is following: 49.7%Ti, 15.3%Zr, 27.2%Ni and 7.8%Cu, while that of the eutectic was 25.0%Ti, 17.7%Zr, 29.5%Ni and 27.8%Cu. One can see that the composition of the eutectic (close to the alloy G1C) lies within the range marked by Lin and Johnson [14]. The measured values of T_g, T_x and T_l allowed to calculate values of $\Delta T_x = 0.58$ for ribbons from the alloy G_0 and 0.59 for the alloy G1C.

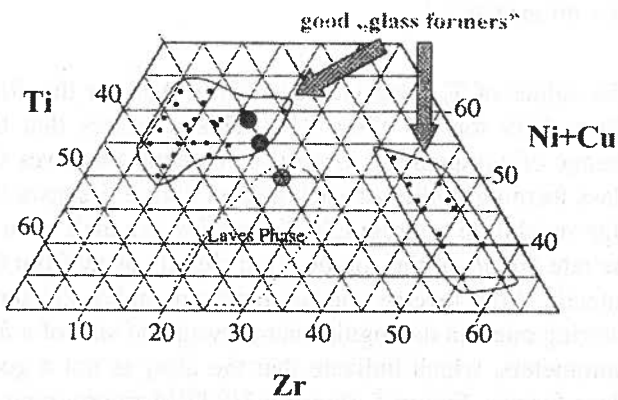

Fig. 2. Quasi ternary phase diagram Ti-Zr-(Ni+Cu) after Lin and Johnson with marked by black dots compositions yielding amorphous structures

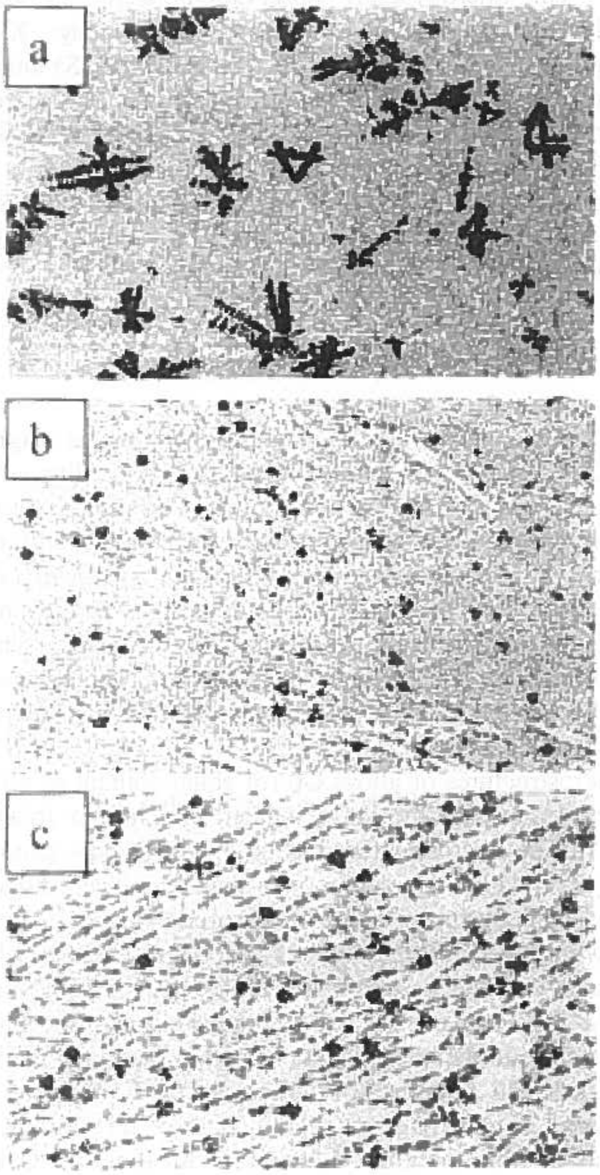

Fig. 3. SEM microstructures of the as iron mould cast alloys G0 (a), G1-1 (b) and G1C (c)

The values of T_{gr} also increased from 0.58 for the alloy G0 to 0.59 for the alloy G1C. This indicates that the change of composition toward the eutectic improves the glass forming ability of such alloys. Figure 4 shows the high resolution micrograph of the alloy G1 melt spun at the rate 10 m/s of the composition slightly away from the eutectic. After reverse Fourier transform and background filtering one can distinguish nanocrystals of size of a few nanometers, which indicate that the alloy is not a good glass former. Figure 5 shows a HRTEM micrograph of alloy G1C, where contrast only from amorphous structure can be seen indicating better glass forming ability of the eutectic alloy.

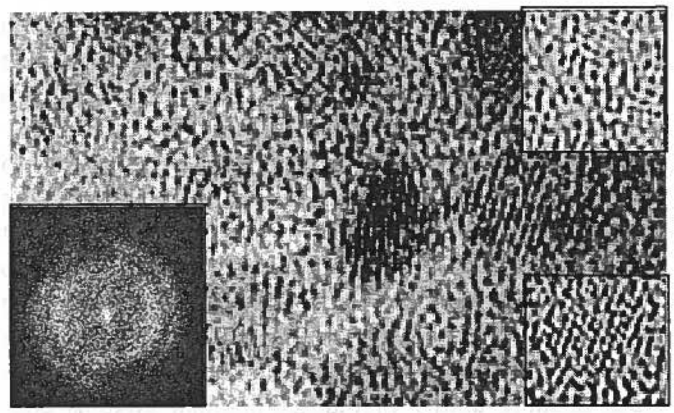

Fig. 4. HRTEM micrograph, its Fourier transform, and noise-removed images as the inserts in corners of the sample G1 melt spun at ~10 m/s

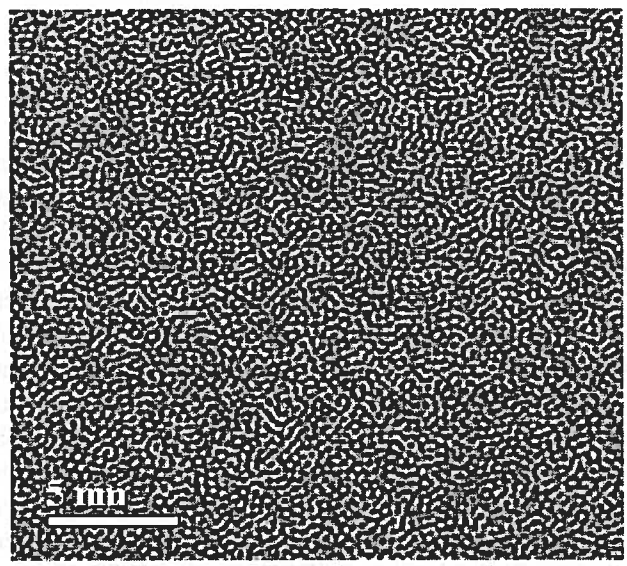

Fig. 5. HRTEM micrograph G1C melt spun at ~10 m/s

Fig. 6 shows a set of SEM micrographs of the alloys G1-1, G1-7 (b) and G1-7A (c) and G1-7AA, where the alloy G1-7 was designed basing on the alloy G1-1 with 10% addition of Mn on the expense of nickel and copper. Subsequent alloys were cast searching for the eutectic composition. One can see that the alloy G1-7 contain a large amount of gray primary crystals and also rectangular dark crystals. Based on the determined composition of the eutectic mixture visible between the primary crystals alloy G1-7A was cast. Its microstructure reveals mostly the eutectic one and only a small amount of the rectangular dark crystals. The alloy G1-7AA showed no rectangular crystals, however eutectic areas are larger, what may indicate a pseudoternary character of the eutectic. In fact a difference between microstructures of alloys G1-7A and G1-7AA is rather small, as their composition difference is not larger than 2 at %. DSC measurements of the T_g, T_x and T_l temperatures allowed to

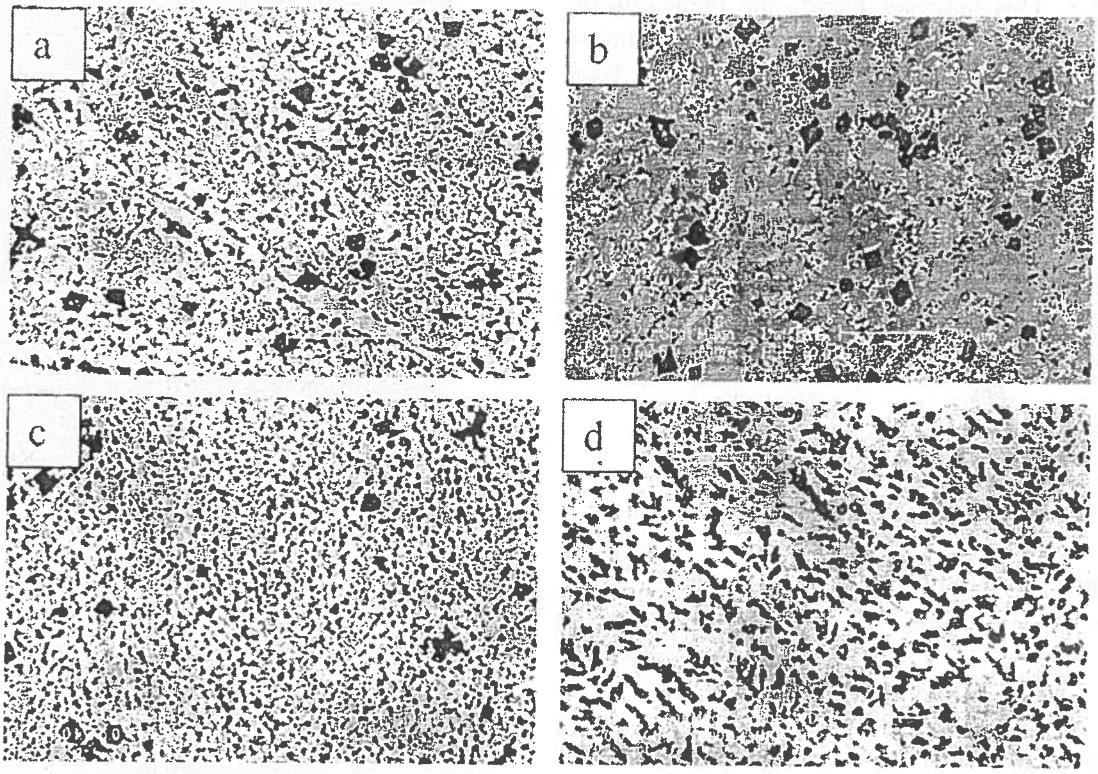

Fig. 6. The scanning microstructure of slowly solidified alloy G1(a), G1-7 (b) and G1-7A (c) and G1-7AA

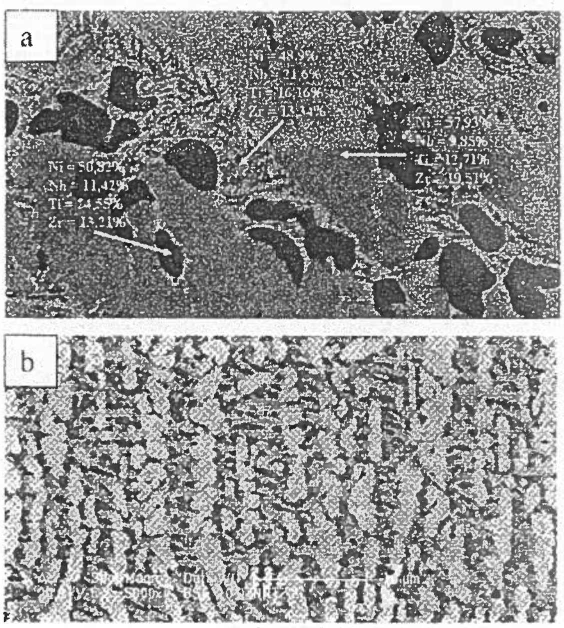

Fig. 7. SEM micrograph of the iron mould cast alloys Ni-1(a) and Ni-2E

determine ΔT_x, equal to 28 and 24 for alloys G1-7A and G1-7AA respectively, while T_{gr} was equal 0.63 and 0.64 respectively. One can see that differences in T_x and T_{gr} were very small and it is difficult to judge the changes of the glass forming ability within this alloy. It might be caused by a very weak glass transition effects difficult to measure. The additions of aluminum to alloy G1-7AA did not cause improvement of the glass forming ability as judged from T_{gr} values [14]. These observations together with studies on manganese additions indicate that the confusion principle was not confirmed in the present studies.

Fig. 7 shows SEM micrographs of alloys NNTZ2 and and NNTZ3. One can see that in the first alloy the gray primary crystals of composition 57.9% Ni, 9.9% Nb, 12.7% Ti and 19.5% Zr constitute large fraction of the volume. There are also black crystals (of composition 50.8% Ni, 11.4% Nb, 24.5% Ti and 13.2% Zr) and a small amount of the eutectic of composition 48.9% Ni, 21.6% Nb, 16.2% Ti and 13.4% Zr. The microstructure of the as cast alloy of composition close to the eutectic (Fig. 7b) shows at higher magnification at least 3 phases within a fine grain mixture indicating eutectic-like structure. The DSC curves of both alloys show strong relaxation effects before the crystallization temperature, starting at 534°C and it is difficult to ascertain the T_g temperature. However, the X-ray diffraction curves obtained from the ribbons cast at 20 m/s from the wheel side and the free side show clear crystallization in the ribbon free side in the alloy NNTZ-2 and no peaks from crystals on both sides from the ribbon taken from the alloy NNTZ-3. This indicates clearly the improvement of the glass forming ability when changing the composition of the quaternary alloy toward the eutectic. This observation is confirmed while taking the HRTEM image (Fig. 9) where no contrast from fringes can be seen confirming X-ray results which indicated the presence of the amorphous phase.

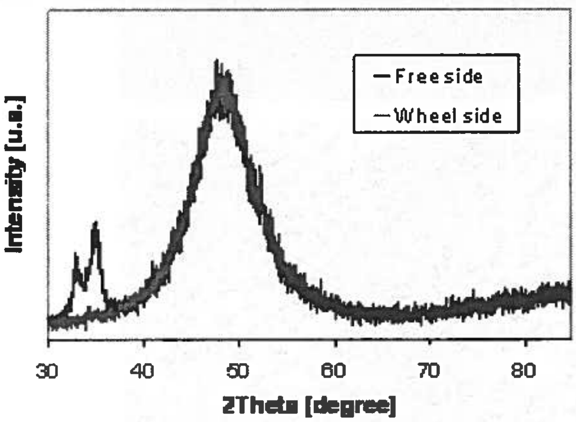

Fig. 8. X-Ray diffraction curve taken from the wheel side (red) and the free side (black) of the melt spun ribbon from the alloy NNTZ2 taken at 22 m/s

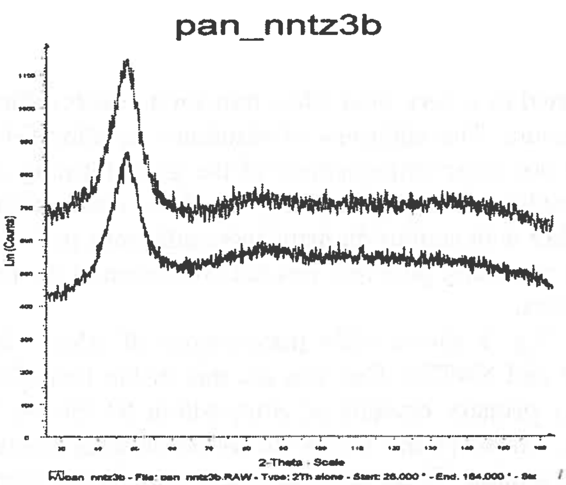

Fig. 8b X-Ray diffraction curve taken from the wheel side (top) and the free side (bottom curve) of the melt spun ribbon from the alloy NNTZ3 taken at 22 m/s

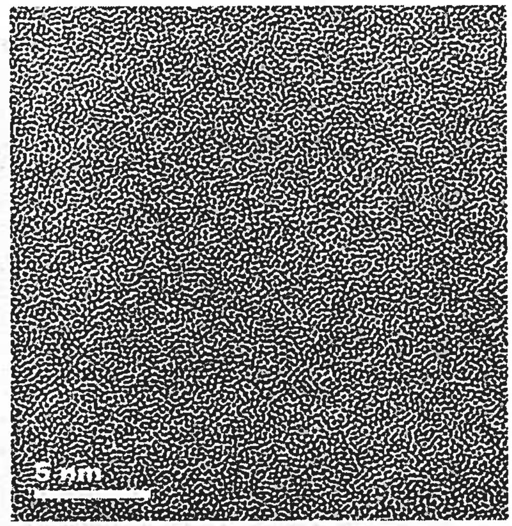

Fig. 9. HRTEM Fourier Filtered image taken from NNTZ3 alloy ribbon cast at 22 m/s

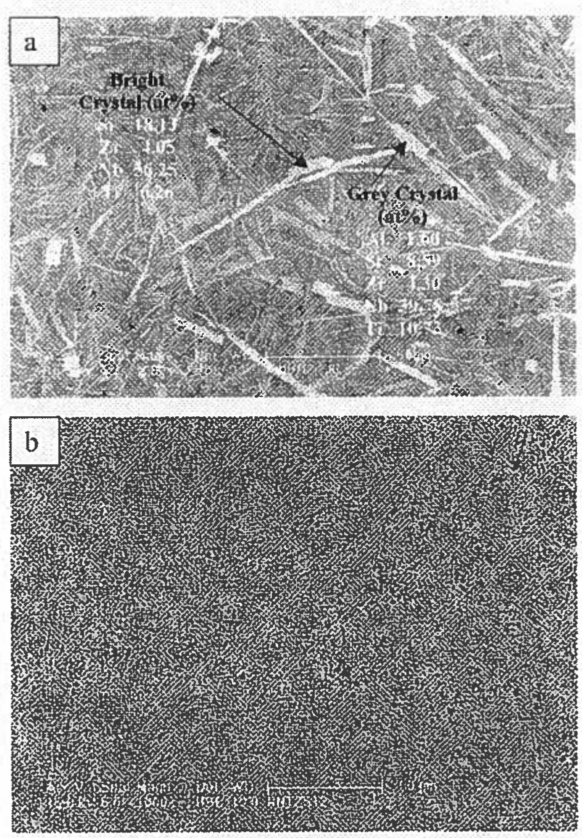

Fig. 10. SEM micrographs of the iron mould cast NNTZ5 alloy (a) and below of the eutectic NNTZS12 (b)

Figure 10 shows SEM micrographs taken from the alloys NNTZS5 and NNTZS12 developed based on the eutectic NNTZ3 alloy by adding silicon as suggested in earlier works [11, 12] that reported a positive role of silicon in glass forming at similar compositions. In the first alloy two types of crystals can be seen; i.e. elongated bright ones of composition 18.1% Si, 4.1% Zr 56.2% Nb, 6.3% Ti and 15.3% Ni and gray ones of composition 1.6% Al., 8.6% Si, 4.3% Zr, 39.8% Nb, 10.7% Ti and 35.0% Ni. One can see that the primary crystals contain a large amount of Nb and Si therefore the content of these elements in the eutectic is much lower. The composition of the eutectic is very close to that of the alloy NNTZS12 (Table 1) which shows indeed fine-grain eutectic-like microstructure. As in the case of alloys NNTZ2 and NNTZ3 the X-ray diffraction trace from alloy NNTZ5 (Figure 11) shows in addition to the broad band from the amorphous structure also small peaks from the crystalline phases indicating only a moderate glass forming ability. DSC curves do not reveal a clear glass transition effect. However, the crystallization peaks are much higher for the eutectic alloy.

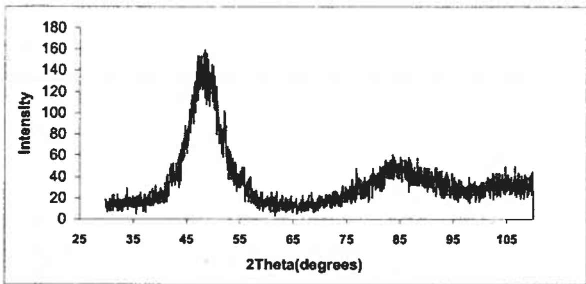

Fig. 11. X-Ray diffraction curve taken from the wheel side of the melt spun ribbon from the alloy NNTZS5 taken at 22 m/s

4. Conclusions

- The TiZrNiCu and NiTiZrNb quaternary eutectic alloys show improved glass forming ability as manifested by ΔT_x which increases from 58 to 60 and an increase of T_{gr} from 0.58 to 0.59 when compared with alloys containing primary crystals. The melt spun ribbons cast from the eutectic alloys did not show nanocrystals compared with alloys showing the presence of primary crystals as detected using the high resolution transmission electron microscopy.
- Additions of a fifth element Mn to TiNiZnNi alloy and Si to the NiTiZrNb alloy do not clearly improves glass forming ability of the quinary eutectics as compared to the quaternary ones. This does not follow the confusion concept which suggest that an increase in the number of the alloying elements should enhance the glass forming ability.

Acknowledgements

The financial support by the European Project **MCRTN-CT-2003-504692** and Polish Ministry of Science and Informatization Project Nr 62/E-88/SPB/6PRUE/DIE420/2004-2007 is gratefully acknowledged.

REFERENCES

[1] J. Dutkiewicz, T. B. Massalski, Metallurgical Transactions **12A**, 773 (1981).
[2] C. Woychik, J. Dutkiewicz, T. B. Massalski, TMS-AIME Meeting on Alloy Phases, Atlanta USA, 6-10 March 1983.
[3] T. B. Massalski, C. G. Woychik, J. L. Murray, Alloy Phase Diagrams Proceedings of Symposium L.H. Bennett, T.B. Massalski, B.C. Giessen ed., p. 241 (1983).
[4] A. Inoue, Bulk Amorphous Alloys; Preparation and Fundamental Characteristics, Trans Tech Publications LTD, Switzerland, 1998.
[5] J. Eckert, Mater. Sci Eng. **A226-228**, 364 (1997).
[6] J. Morgiel, M. Faryna, W. Maziarz, T. Czeppe, P. Ochin P. J. Dutkiewicz, Inżynieria Materiałowa **25**, 224-227 (2004).
[7] J. Morgiel, P. Ochin, Foundation of Materials Design, ed. P. Zięba, Research Signpost (in print).
[8] A. L. Greer, Nature **366**, 303 (1993).
[9] J. Morgiel, T. Czeppe, W. Maziarz, Ł. Major, P. Ochin, S. Anastasova, J. Dutkiewicz, Proceedings of Conference Metalurgia, Krynica, ed. Committee of Metallurgy PAN p. 453 (2006).
[10] S. Pang, T. Zhang, K. Asami, A. Inoue, Mater. Sci. Eng.: A **375-377**, 368-371 (2004).
[11] S. Pang, T. Zhang, K. Asami, A. Inoue, Mater. Sci. Eng.: A **375-377**, 368-371 (2004).
[12] M. H. Lee, J. Y. Lee, D. H. Bae, W. T. Kim, D. J. Sordelet, D. H. Kim, Intermetallics **12**, 1133-1137 (2004).
[13] J. K. Lee, D. H. Bae, S. Yi, W. T. Kim, D. H. Kim, Journal of Non-Crystalline Solids **333**, 212-220 (2004).
[14] X. H. Lin, W. L. Johnson, J.Appl. Phys. **78**, 6513 (1995).

Received: 20 September 2006.